Sensitivity of inverse estimation of 2004 elemental carbon emissions inventory in the United States to the choice of observational networks

Yongtao Hu[1], Sergey L. Napelenok[2], M. Talat Odman[1] and Armistead G. Russell[1]

[1]School of Civil and Environmental Engineering, Georgia Institute of Technology, Atlanta, Georgia, USA

[2]National Exposure Research Laboratory, U.S. Environmental Protection Agency, Research Triangle Park, North Carolina, USA

Abstract

Choice of observational networks used for inverse re-estimation of elemental (or black) carbon (EC) emissions in the United States impacts results. We convert the Thermal Optical Transmittance (TOT) EC measurements to the Thermal Optical Reflectance (TOR) equivalents to make full utilization of available networks in inverse modeling of EC using regional air quality model. Results show that using the Interagency Monitoring of Protected Visual Environments (IMPROVE) network gives significantly lower emissions estimate compared to using the Speciation Trends Network (STN) and other networks or using all available networks together. The re-estimate obtained by using IMPROVE sites alone made overall model performance worse compared to the bottom-up estimate of EC emissions, while both re-estimates, using STN (and others) sites and using all sites together, significantly improved the performance. Further analysis suggests that site density with respect to geographical location (downwind) impacts the robustness of a network's inverse re-estimate.

1. Introduction

Atmospheric chemical transport models are subject to emissions uncertainties. Application of inverse methods in atmospheric models helps reconcile the gap between modeled and observed species concentrations by adjusting the emissions. During the past decade, using surface monitoring networks and satellite images, inverse modeling has been actively utilized to "correct" bottom-up emissions estimates [*Bergamaschi et al.*, 2000; *Elbern et al.*, 2000; *Gilliland et al.*, 2003; *Heald et al.*, 2004; *Mendoza-Dominguez and Russell*, 2001]. However, the adoption of different observational networks in inverse modeling can lead to discrepancies in inverse emissions estimates [*Law et al.*, 2003; *Patra et al.*, 2006]. Of interest is the sensitivity of the inverse estimates to the choice of observational networks. Here we study the sensitivity of inverse estimation of elemental (or black) carbon (EC) emissions to different observational networks and examine the robustness of the re-estimates.

EC is measured as the light-absorbing fraction of carbonaceous aerosol species and can be a significant component of fine particulate matter ($PM_{2.5}$). However, its measurement is operationally defined and different measurement techniques give differing, but often highly correlated results [*Chow et al.*, 2004; *Hitzenberger et al.*, 2006; *Nejedlÿ et al.*, 2003; *Schmid et al.*, 2001]. EC is found to be associated with adverse human health effects and regional visibility degradation and can influence radiative forcing [*Charlson et al.*, 1992; *Penner et al.*, 1992; *Ramanathan et al.*, 2001]. EC in the atmosphere comes solely from combustion processes of either fossil fuels (e.g. coal burning and diesel combustion) or bio-mass (e.g. wildfire and prescribed burning). Studies suggest EC emissions inventories are significantly underestimated at regional

47 level (e.g. in the United States) [*Eder and Yu*, 2006; *Tesche et al.*, 2006]. Limited inverse
48 modeling studies have been carried out to adjust the existing emissions inventory
49 [*Hakami et al.*, 2005; *Park et al.*, 2003] utilizing aircraft and/or surface measurements,
50 however the spatial and temporal coverage of EC measurements were extremely limited
51 in these studies.

52 EC emissions in the US are estimated to be about 0.4 Tg yr^{-1} which is 5% of the
53 global totals [*Bond et al.*, 2004], which makes the US the third largest emitter after China
54 (~20%) and India (~9%). There are two major national surface networks measuring EC
55 currently operational in the US: the Interagency Monitoring of Protected Visual
56 Environments (IMPROVE) network and the Speciation Trends Network (STN). In
57 addition, there is the SouthEastern Aerosol Research and CHaracterization (SEARCH)
58 [*Hansen et al.*, 2006] in the southeastern US, and the Assessment of Spatial Aerosol
59 Composition in Atlanta (ASACA) [*Butler et al.*, 2003] in Georgia, measuring EC as well.
60 IMPROVE sites are located primarily in rural areas while STN, SEARCH and ASACA
61 networks include urban, sub-urban and rural sites (urban and sub-urban sites being the
62 majority). The observations at rural sites (i.e. a portion of current IMPROVE sites) have
63 been utilized by *Park, et al.* [2003] to adjust the carbonaceous aerosols including EC
64 emissions in the US for 1998, but urban networks have not been utilized in previous
65 similar inverse modeling studies.

66 We adopt an inverse method [*Mendoza-Dominguez and Russell*, 2000], along with
67 the Community Multiscale Air Quality model (CMAQ) [*Byun and Schere*, 2006]
68 equipped with the Decoupled Direct Method in Three Dimensions (DDM-3D) [*Cohan et*
69 *al.*, 2005; *Dunker et al.*, 2002; *Napelenok et al.*, 2006; *Yang et al.*, 1997] for sensitivity

70 calculations, to adjust the 2004 US regional EC emissions inventory. We examine the
71 sensitivity of EC emissions adjustment to the choice of different observational networks
72 (i.e., IMPROVE versus STN, SEARCH and ASACA combined (called SSA hereafter)
73 and all of the networks (called ALL hereafter) (see site locations in Figure 1a)) in the
74 inverse modeling.

75 ## 2. Method

76 For five chosen months (January, March, May, August and October) in 2004, we
77 apply CMAQ (Version 4.5, updated with mass conservation [*Hu et al.*, 2006]) to simulate
78 EC concentrations as well as DDM-3D to obtain coefficients of EC sensitivity to specific
79 sources. The modeling domain (Figure 1b), covering the entire continental US as well as
80 portions of Canada and Mexico, has a 36-km horizontal resolution and thirteen vertical
81 layers extending ~16 km above ground, 7 layers below 1 km and a first layer of 18 m
82 thickness. The Fifth-Generation PSU/NCAR Mesoscale Model (MM5) [*Grell et al.*, 1994]
83 is used to develop the meteorological fields and is run with 34 vertical layers using four
84 dimensional data assimilation (FDDA) technique and the Pleim-Xiu Land-Surface Model
85 (PX-LSM) [*Pleim and Xiu*, 1995; *Xiu and Pleim*, 2001]. Simulated surface
86 meteorological fields were examined against surface hourly observations from North
87 America (Table S1), with performance well within the typical range for air quality
88 modeling [*Emery et al.*, 2001; *Hanna and Yang*, 2001]. The Sparse Matrix Operator
89 Kernel Emissions (SMOKE) model [*CEP*, 2003] is used to prepare gridded, CMAQ-
90 ready emissions using *a priori* emissions (APRIORI) for the year 2004 which were
91 projected from a 2002 inventory (VISTAS2002) [*MACTEC*, 2005]. Biomass fire
92 emissions in VISTAS2002 were estimated for a "typical" year by averaging actual fire

93 information from a five-year period between 1999 and 2003, which is used directly as the
94 estimate for 2004. We sub-divide APRIORI to twenty-seven sources: Canadian total
95 within the domain, Mexican total within the domain, and the continental US emissions
96 divided to five regional planning organization (RPO) regions (Figure 1b), further split
97 into five categories: on-road mobile, off-road mobile, fire (including wildfire, agricultural
98 burning and prescribed burning), wood fuel and "others" (including coal-burning power
99 plants etc.). We calculate the sensitivity of EC concentrations (at each grid cell) to each
100 of the above sub-group EC emissions sources.

101 Sensitivities of EC concentration to each individual sub-group source are used to
102 estimate how much EC emissions from each specific source should be adjusted to
103 minimize the CMAQ EC prediction errors (difference between the simulation and the
104 observation) at each site through ridge regression [*Draper and van Nostrand*, 1979].
105 Detailed description of the inverse method is documented elsewhere [*Mendoza-*
106 *Dominguez and Russell*, 2000]. Here, we calculate the emissions adjustment factors
107 m that minimize the objective function Γ (Equations S1 and S2) which is a linear
108 combination of the errors and the adjustments to emissions.

109 Inverse modeling is conducted three times using measurements, respectively, from
110 the IMPROVE, SSA and ALL networks. Measurements used here are 24-hr averages
111 (midnight to midnight) collected using filters, but in different frequencies, either daily, or
112 every third day or sixth day. We first average all measurements (and the corresponding
113 predictions as well as the sensitivity coefficients) at the same site to get a monthly mean.
114 For multiple sites that are located in the same grid cell, we further average their monthly
115 means to obtain a composite. After merging, the number of IMRPOVE sites remained the

same at 163 (i.e. no multiple sites in a same grid cell), while the number of SSA sites dropped from 245 to 211. Note that different protocols are adopted by the networks to measure aerosol carbon fraction (EC and organic carbon (OC)): the Thermal Optical Transmittance (TOT) is used by STN and ASACA while the Thermal Optical Reflectance (TOR) is used by IMPROVE and SEARCH. Most of the speciation profiles used in SMOKE to split EC and OC emissions from $PM_{2.5}$ totals were determined using the TOR protocol. For consistency, we convert the TOT measurements to TOR equivalent values by using seasonal factors (Table 1) obtained through a parallel TOR and TOT comparison study recently carried out at the SEARCH sites [*Chen et al.*, 2009].

We apply three sets of adjustment factors to APRIORI to obtain the posterior EC emissions inventories. These re-estimates of emissions are then used to drive the model. We calculate the improvements of the posterior CMAQ model performance (with respect to the prior performance) to examine the robustness of each re-estimate obtained. Model performance is judged by the fractional bias (FB) and fractional error (FE) (Equations S3 and S4).

3. Results and Discussion

APRIORI estimates (through bottom-up methods) the US continental total EC emissions for 2004 as about 0.36 Tg yr^{-1}. Off-road and fire emissions are the two leading categories continent-wide (Figure S1a). Fire emissions lead in the west (WRAP and CENRAP) and off-road emissions lead in the east (VISTAS, MANE-VU and Midwest). By using APRIORI, the model performance is comparable to what is typically reported for regional application of CMAQ [*Eder and Yu*, 2006; *Tesche et al.*, 2006]. Overall FB and FE against ALL sites are -42.6% and 65.1%. Among the five simulated months: the

139 best performance is seen for winter (January) and the worst for summer (August) though
140 all of the months were biased low (Figure 2). Note that CMAQ predictions did a slightly
141 better job at the IMPROVE sites than at the SSA sites (not shown), while on average, the
142 IMPROVE sites have much cleaner air than the SSA sties with an observed EC mean of
143 0.23 $\mu g\ m^{-3}$ versus 1.05 $\mu g\ m^{-3}$.

144 We re-estimate the US continental total EC emissions for 2004 to be 0.40, 0.29 and
145 0.44 $Tg\ yr^{-1}$, respectively, by using ALL, IMPROVE and SSA networks in the inversion.
146 Note that we apply the adjustment factors to APRIORI for each month of 2004, i.e. either
147 the chosen month itself or a month that the chosen month represents (Table S2), to get the
148 annual totals. Overall, the IMPROVE re-estimate reduced the prior annual emissions
149 significantly, while both the ALL and SSA re-estimates increased the emissions. Between
150 the ALL and SSA re-estimates, insignificant differences (within a few percents) are seen
151 for most RPOs and categories, but the SSA re-estimates increased emissions largely from
152 WRAP and from fire while the ALL re-estimates did not (Figure S1). Both the ALL and
153 SSA re-estimates improved model performance (against ALL sites) for all five months,
154 for both FB and FE (Figure 2). However the IMPROVE re-estimate led to a deterioration
155 in the model performance (Figure 2). We also calculated "performance change" (defined
156 as the difference of FEs between the posterior and the prior) at each individual site. Both
157 the ALL and SSA re-estimates resulted in better CMAQ predictions at about 70% of the
158 total sites (i.e. ALL sites), while the IMPROVE re-estimate made predictions worse at
159 two thirds of them (Figure S2), roughly proportional to the number of SSA and
160 IMPROVE sites. This suggests that the IMPROVE re-estimate of EC emissions is less
161 robust than the ALL or SSA re-estimate. This is tied to the geographic location of major

emission sources and the monitors. While one set of sources (on-road, off-road and fuel burning) are concentrated in urban areas (similar to SSA sites), fires are not. Thus using a network that is less sensitive to the one set of sources weakens the inversion.

Prediction errors still remain in the posterior model results obtained by using the ALL and SSA re-estimates even though the performance improved. The remaining errors could come from model parameterization and other model inputs, e.g. errors in vertical diffusion, wind fields, boundary conditions and etc., as well as remaining errors in emissions inputs, e.g. the errors in the temporal variations and sub-regional spatial variability that our emissions adjustments did not address. The remaining prediction errors might also come from the representativeness of point measurements within a modeled grid, especially for sites near polluted areas where large spatial gradients exist in EC concentrations. However, compared to the much coarser grid spacing adopted in previous studies (e.g. 80-km or even 2° latitude by 2.5° longitude), the 36-km grid spacing we have adopted in this study better captures the spatial gradients of primary pollutants like EC.

A common belief is that an inverse re-estimate would be more robust when using a higher density of monitoring sites, especially for primary pollutants like EC. Domain wide, the total number of SSA sites is just slightly larger than IMRPOVE sites, which explains only part of the difference in robustness. However, the monitoring site densities are geographically imbalanced for both the SSA and IMPROVE networks. The IMPROVE sites are situated more in the western US than in the east, while the SSA sites are predominantly in the east (Table 2). Since upper level winds are mostly eastward the urban-oriented SSA network is impacted by emissions from more upwind regions. The

185 life time of EC is about 6 days on average [*Park et al.*, 2005] which is sufficient to be
186 transported across the continent. This can be seen more clearly through the non-zero
187 sensitivity counts reported by RPO region (Table 3a). Monitoring sites located in WRAP
188 are situated in the far west and are having a smaller number of non-zero sensitivities than
189 any other RPO to the east. Inside WRAP the ratio of IMPROVE sites to SSA sites is
190 almost 3:1. Downwind, the number of non-zero sensitivities becomes larger while at the
191 same time the number of SSA sites relative to IMRPOVE sites increase. These results
192 suggest that the robustness of the EC inverse re-estimates are impacted by site density
193 and geographical location, with further downwind sites adding robustness. Furthermore,
194 sites with larger sensitivities receive heavier weightings in inversion (Equation S2). In
195 this regard the location of rural (impacted by smaller sources) vs. urban (impacted by
196 larger sources), plays a role. The sites, that is immediately downwind of larger sources
197 are more impacted and weight more in the inversion. While there is no difference in the
198 average number of non-zero sensitivities between IMPROVE and SSA networks from the
199 same RPO (Table 3a), the average number of above-EC-detection-limit sensitivities are
200 significantly less for IMPROVE than SSA, and more so in the West (Table 3b). This
201 suggests that the robustness of the EC inverse re-estimates is further impacted by the sites
202 located immediately downwind of larger sources. This also explains that the ALL re-
203 estimate was not significantly more robust than the SSA re-estimate though utilizing
204 more than 50% more sites.

205 *Park, et al.* [2003], the only previous top-down estimation of EC emissions in the US,
206 increased the *a priori* estimate of 0.66 Tg yr^{-1} to 0.75 Tg yr^{-1}. They estimated a 15%
207 increase in fossil fuel emissions, a 65% increase in biofuel emissions and a 17% decrease

208 in biomass burning emissions. There are a number of differences between that study and
209 the one presented here. The prior inventory of fossil fuel emissions (totaling to 0.52 Tg
210 yr^{-1}) used in their study had been developed for 1984 [*Cooke et al.*, 1999] and may have
211 largely overestimated the EC fossil fuel emissions for the year 1998 [*Bond et al.*, 2004].
212 Second, the grid spacing was 2° latitude by 2.5° longitude in their global transport model.
213 Third, only 45 rural-sites from IMPROVE network were available then. Finally among
214 the 45 sites, seven of them (model overestimated at these sites) were further excluded.

215 ## 4. Conclusion

216 Our sensitivity study of inverse re-estimation of EC emissions in the US to the
217 choice of different observational networks found that the re-estimate using the
218 IMPROVE sites (all rurally situated) alone leads to significantly different results than
219 using STN sites plus SEARCH and ASACA sites (mainly urban and suburban) or using
220 all sites together. The difference in model performance between the posterior and prior
221 simulations suggests that the IMRPOVE re-estimate was less robust than the other two.
222 Further analysis based on examining the sensitivity coefficients obtained through DDM-
223 3D calculations suggests that it was neither the rural vs. urban site locations nor number
224 of sites, alone, but the site density with respect to geographical location (downwind of
225 source) affected the robustness of the inverse re-estimate as well. Since much of the EC
226 emissions are associated with sources more concentrated in urban areas, having more
227 measurements in urban area leads to better constraining on EC emissions inventory.

228 **Acknowledgements** This work was funded by U.S. Environmental Protection
229 Agency under Grants R-82897601, RD83096001, and RD83107601 and by Georgia
230 Power.

231 REFERENCES

232

233 Bergamaschi, P., et al. (2000), Inverse modeling of the global CO cycle 1. Inversion of
234 CO mixing ratios, *Journal of Geophysical Research*, *105*(D2, 1909-1927).

235 Bond, T. C., et al. (2004), A technology-based global inventory of black and organic
236 carbon emissions from combustion, *Journal of Geophysical Research*, *109*, D14203,
237 doi:14210.11029/12003JD003697.

238 Butler, A. J., et al. (2003), Daily sampling of PM2.5 in Atlanta: Results of the first year
239 of the Assessment of Spatial Aerosol Composition in Atlanta study, *J. Geophys. Res.*,
240 *108*(D7), 8415,doi:8410.1029/2002JD002234.

241 Byun, D., and K. L. Schere (2006), Review of the Governing Equations, Computational
242 Algorithms, and Other Components of the Models-3 Community Multiscale Air Quality
243 (CMAQ) Modeling System, *Applied Mechanics Reviews*, *59*(2), 51-77.

244 CEP (2003), Sparse Matrix Operator Kernel Emissions Modeling System (SMOKE) User
245 Manual, edited, Carolina Environmental Program - The University of North Carolina at
246 Chapel Hill, Chapel Hill, NC.

247 Charlson, R. J., et al. (1992), Climate Forcing by Anthropogenic Aerosols, *Science*, *255*,
248 No. 5043, 5423-5430.

249 Chen, Y., et al. (2009), Comparison of two carbon measurement methods in aerosols in
250 the Southeastern United States, *Manuscript in preparation*.

251 Chow, J. C., et al. (2004), Equivalence of Elemental Carbon by Thermal/Optical
252 Reflectance and Transmittance with Different Temperature Protocol, *Environmental*
253 *Science & Technology*, *38*, 4414-4422.

254 Cohan, D. S., et al. (2005), Nonlinear response of ozone to emissions: source
255 apportionment and sensitivity analysis, *Environmental Science and Technology*, *39*,
256 6739-6748.

257 Cooke, W. F., et al. (1999), Construction of a 1°x1° fossil fuel emission data set for
258 carbonaceous aerosol and implementation and radiative impact in ECHAM4 model,
259 *Journal of Geophysical Research*, *104*, D18, 22,137-122,162.

Draper, N. R., and R. C. van Nostrand (1979), Ridge regressions and James-Stein estimation review and comments, *Technometrics*, *21*, 451-466.

Dunker, A. M., et al. (2002), Comparison of source apportionment and source sensitivity of ozone in a three-dimensional air quality model, *Environmental Science & Technology*, *36*, 2953-2964.

Eder, B., and S. Yu (2006), A performance evaluation of the 2004 release of Models-3 CMAQ, *Atmospheric Environment*, *40*, 4811-4824.

Elbern, H., et al. (2000), 4D-variational data assimilation with an adjoint air quality model for emission analysis, *Environmental Modeling & Software*, *15*, 539-548.

Emery, C., et al. (2001), Enhanced meteorological modeling and performance evaluation for two Texas ozone episodes, Prepared for the Texas Natural Resource Conservation Commissions, ENVIRON International Corporation, Novato, CA

Gilliland, A. B., et al. (2003), Seasonal NH3 emission estimates for the eastern United States based on ammonium wet concentrations and an inverse modeling method, *Journal of Geophysical Research*, *108*, D15, 4477, doi:4410.1029/2002JD003063.

Grell, G., et al. (1994), A description of the Fifth-Generation Penn State/NCAR Mesoscale Model (MM5), NCAR Technical Note: NCAR/TN-398+STR.

Hakami, A., et al. (2005), Adjoint inverse modeling of black carbon during the Asian Pacific Regional Aerosol Characterization Experiment, *Journal of Geophysical Research-Atmospheres*, *110*, D14301,doi:14310.11029/12004JD005671.

Hanna, S. R., and R. Yang (2001), Evaluations of mesoscale models' simulations of near-surface winds, temperature gradients, and mixing depths, *Journal of Applied Meteorology*, *40*, 1095-1104.

Hansen, D. A., et al. (2006), The Southeastern Aerosol Research and Characterization Study, part 3: Continuous measurements of fine particulate matter mass and composition, *J. Air & Waste Manage. Assoc.*, *56(9)*, 1325-1341.

287 Heald, C. L., et al. (2004), Comparative inverse analysis of satellite (MOPITT) and
288 aircraft (TRACE-P) observations to estimate Asian sources of carbon monoxide, *Journal*
289 *of Geophysical Research*, *109*(D23306), doi:10.1029/2004JD005185.

290 Hitzenberger, R., et al. (2006), Intercomparison of Thermal and Optical Measurement
291 Methods for Elemental Carbon and Black Carbon at an Urban Location *Environmental*
292 *Science & Technology*, *40*, 6377-6383.

293 Hu, Y., et al. (2006), Mass conservation in the Community Multiscale Air Quality model,
294 *Atmospheric Environment*, *40*, 1199-1204.

295 Law, R. M., et al. (2003), TransCom 3 CO2 inversion intercomparison: 2. Sensitivity of
296 annual mean results to data choices, *Tellus Series B-Chemical And Physical Meteorology*,
297 *55B*(580-595).

298 MACTEC (2005), Documentation of the Revised 2002 Base Year, Revised 2018, and
299 Initial 2009 Emission Inventories for VISTAS, edited, Visibility Improvement State and
300 Tribal Association of the Southeast (VISTAS).

301 Mendoza-Dominguez, A., and A. G. Russell (2000), Iterative Inverse Modeling and
302 Direct Sensitivity Analysis of a Photochemical Air Quality Model, *Environmental*
303 *Science & Technology*, *34*, 4974-4981.

304 Mendoza-Dominguez, A., and A. G. Russell (2001), Estimation of emission adjustments
305 from the application of four-dimensional data assimilation to photochemical air quality
306 modeling, *Atmospheric Environment*, *35*, 2879-2894.

307 Napelenok, S. L., et al. (2006), Decoupled Direct 3D Sensitivity Analysis For Particulate
308 Matter (DDM-3D/PM), *Atmospheric Environment*, *40*, 6112-6121.

309 Nejedlÿ, Z., et al. (2003), Evaluation of Elemental and Black Carbon Measurements from
310 the GAViM and IMPROVE Networks, *Aerosol Science and Technology*, *37*, 96-108,
311 doi:110.1080/02786820390112498.

312 Park, R. J., et al. (2003), Sources of carbonaceous aerosols over the United States and
313 implications for natural visibility, *Journal of Geophysical Research-Atmospheres*, *108*,
314 D12,4335,doi:4310.1029/2002JD003190.

315 Park, R. J., et al. (2005), Export efficiency of black carbon aerosol in continental outflow:
316 Global implications, *Journal of Geophysical Research-Atmospheres*, *110*, D11205,
317 doi:11210.11029/12004JD005432.

318 Patra, P. K., et al. (2006), Sensitivity of inverse estimation of annual mean CO2 sources
319 and sinks to ocean-only sites versus all-sites observational networks, *Geophysical*
320 *Research Letters*, *33*, L05814, doi:05810.01029/02005GL025403.

321 Penner, J. E., et al. (1992), Effects of Aerosol from Biomass Burning on the Global
322 Radiation Budget, *Science*, *256*, 1432-1434.

323 Pleim, J. E., and A. Xiu (1995), Development and testing of a surface flux and planetary
324 boundary layer model with explicit soil moisture parameterization for application in
325 mesoscale models, *Journal of Applied Meteorology*, *34*, 16-32.

326 Ramanathan, V., et al. (2001), Aerosols, climate, and the hydrological cycle, *Science*, *294*,
327 2119-2124.

328 Schmid, H., et al. (2001), Results of the "carbon conference" international aerosol carbon
329 round robin test stage I, *Atmospheric Environment*, *35*, 2111-2121.

330 Tesche, T. W., et al. (2006), CMAQ/CMAx annual 2002 performance evaluation over the
331 eastern US, *Atmospheric Environment*, *40*(4906-4919).

332 Xiu, A., and J. E. Pleim (2001), Development and application of a land-surface model. I:
333 Application in a mesoscale meteorology model, *Journal of Applied Meteorology*, *40*,
334 192-209.

335 Yang, Y.-J., et al. (1997), Fast, direct sensitivity analysis of multidimensional
336 photochemical models, *Environmental Science and Technology 31*, 2859-2868.
337
338
339 ## Figure Captions

340 **Figure 1.** (a) EC monitoring networks: IMPROVE (green dots), STN (red dots) and

341 SEARCH and ASACA (pink dots). Urban areas in the United States are shown in blue.

342 (b) Modeling domain, with a 36-km horizontal grid spacing. The sub regions of the

United States studied as source areas in the sensitivity analysis are the five RPO regions: CENRAP, Midwest RPO, MANE-VU, WRAP and VISTAS.

Figure 2. Monthly CMAQ EC performance (against ALL sites) by using the *a priori* and the three *a posteriori* emissions inventories (i.e. the All, IMPROVE and SSA re-estimates): (a) FB and (b) FE.

Tables

Table 1 Seasonal factors (a) converting BC ambient concentration from TOT measurements to TOR equivalents: $TOR = a \times TOT$.

Winter	Spring	Summer	Fall
1.672	1.831	2.577	1.890

*Data source *Chen et al.* [2009]

Table 2 Sites numbers located in each RPO region.

Network	WRAP	CENRAP	Midwest RPO	VISTAS	MANE-VU	Total
SSA	35	39	34	67	36	211
IMPROVE	92	24	7	17	23	163
ALL	124	60	39	82	53	358

*These are numbers of composite sites.

Table 3a Average number of non-zero DDM-3D sensitivities (below 0.000001 $\mu g\ m^{-3}$ per total EC emissions in a specific source is considered numerical noise and omitted).

Network	WRAP	CENRAP	Midwest RPO	VISTAS	MANE-VU	Domain
SSA	11.7	23.0	24.6	26.3	27.0	23.0
IMPROVE	11.4	21.7	25.4	26.8	27.0	17.2
All	11.5	22.6	24.7	26.4	27.0	20.4

361 **Table 3b** Average number of above-EC-detection-limit DDM-3D sensitivities

362 (>0.05μg m^{-3} per total EC emissions in a specific source).

Networks	WRAP	CENRAP	Midwest RPO	VISTAS	MANE-VU	Domain
SSA	2.5	1.7	2.4	2.8	2.8	2.5
IMPROVE	0.7	0.8	1.9	1.8	2.0	1.1
All	1.2	1.4	2.2	2.6	2.4	1.8

363

(a)

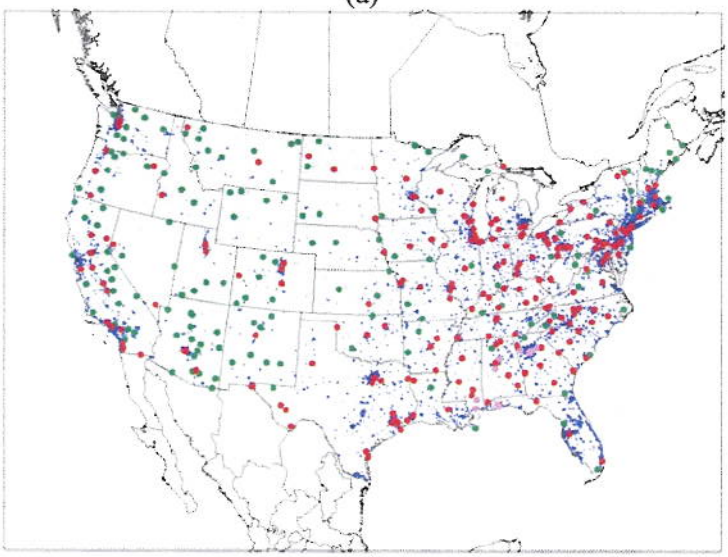

(b)

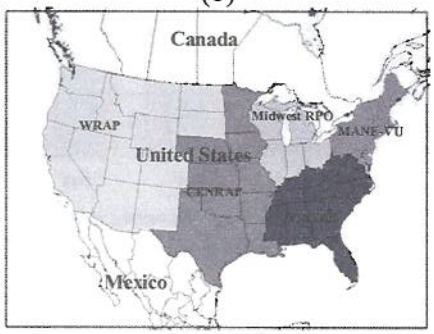
Canada
WRAP
Midwest RPO
MANE-VU
United States
CENRAP
Mexico

Figure 1

(a)

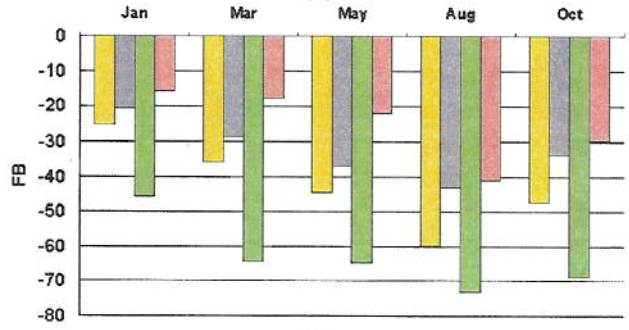
Jan
Mar
May
Aug
Oct
0
-10
-20
-30
-40
-50
-60
-70
-80
FB

(b)

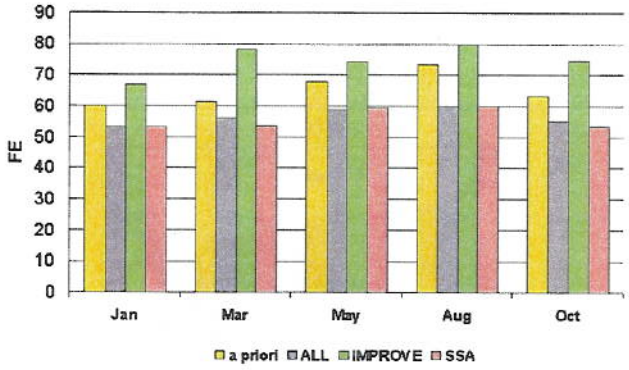
90
80
70
60
50
40
30
20
10
0
FE
Jan
Mar
May
Aug
Oct
a priori
ALL
IMPROVE
SSA

Figure 2

Supporting Material

Table S1 Statistical measures in MM5-generated meteorological parameter fields with respect to the Techniques Development Laboratory (TDL) surface observations.

Parameters	Measures	Unit	Jan	Mar	May	Aug	Oct
Surface Wind Speed	Mean OBS	(m/s)	3.72	4.01	3.87	2.89	3.25
	Bias	(m/s)	-0.01	-0.14	-0.08	0.07	0.13
	RMSE	(m/s)	2.02	1.98	1.89	1.73	1.81
Surface Wind Direction	Mean OBS	(deg)	261.25	243.56	211.28	227.50	193.77
	Bias	(deg)	2.56	2.39	2.01	2.48	2.57
	Gross Error	(deg)	25.98	26.92	28.77	32.61	27.80
Surface Air Temperature	Mean OBS	(K)	270.63	280.34	289.54	293.92	285.95
	Bias	(K)	-0.79	-0.75	-0.29	-0.24	-0.36
	RMSE	(K)	3.23	2.94	2.63	2.49	2.46
Surface Humidity	Mean OBS	(g/kg)	3.33	5.04	8.68	11.55	7.71
	Bias	(g/kg)	0.01	0.09	-0.11	-0.22	-0.15
	Gross Error	(g/kg)	0.52	0.77	1.10	1.28	0.92

Table S2 Representative months and the months they represent.

Representing	Jan	Mar	May	Aug	Oct
Represented	Dec and Feb	Apr	Jun	Jul and Sep	Nov

Equations

We calculate the emissions adjustment factors m that minimize the objective function Γ:

$$\Gamma = e^T W_e e + m^T W_m m \quad \text{(S1)}$$

$$m = \left(G^T W_e G + W_m\right)^{-1} G^T W_e d \quad \text{(S2).}$$

where e is a vector of length N representing the prediction errors remaining after adjustment of emissions (N being the total number of valid pairs of observation and simulation during each chosen month), m is the vector of factors that are used to adjust each sub-group emission source and is of length J (J being the total number of emissions sub-groups: 27), superscript T denotes the transpose of a vector or matrix, W_e is a N×N matrix weighting the observations, W_m is a J×J matrix representing the penalty function

that constrains the emissions adjustment factors within prescribed bounds derived from the uncertainty limits of the base emission estimates, G is a N×J matrix of semi-normalized sensitivity coefficients and d is vector of current prediction errors before the emissions adjustments and is of length N. The first term of our objective function is the square of the weighted prediction error while the second term is the square of the penalized emissions adjustment. The linear system described by Equation 2 has a dimension of N with J unknown parameters. When N >J, such as the cases in this study, this is an over-determined problem, and will have a unique least square solution.

Model performance is judged by the fractional bias (FB) and fractional error (FE):

$$FB = \frac{1}{N}\sum_{i=1}^{N}\frac{2(Sim_i - Obs_i)}{(Sim_i + Obs_i)} \times 100\% \quad \text{(S3)}$$

$$FE = \frac{1}{N}\sum_{i=1}^{N}\frac{2|Sim_i - Obs_i|}{(Sim_i + Obs_i)} \times 100\% \quad \text{(S4)}$$

where N is the total number of valid pairs of simulated (Sim) and observed (Obs) concentrations.

Figure Captions

Figure S1. EC emission totals of the *a priori* and the *a posteriori* inventories (i.e. the ALL, IMPROVE and SSA re-estimates): (a) by category (continental US) and (b) by region.

Figure S2. "Performance change" (against ALL sites) versus percentage of total number of sites (one count at each month).

(a)

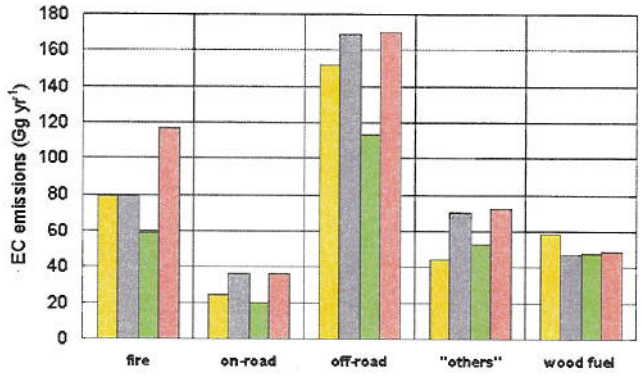

(b)

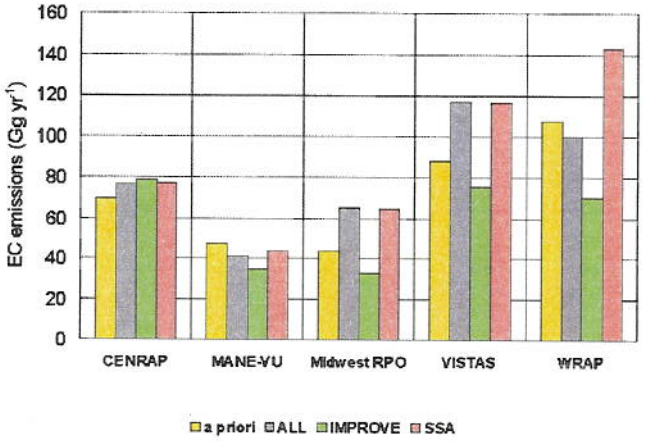

Figure S1

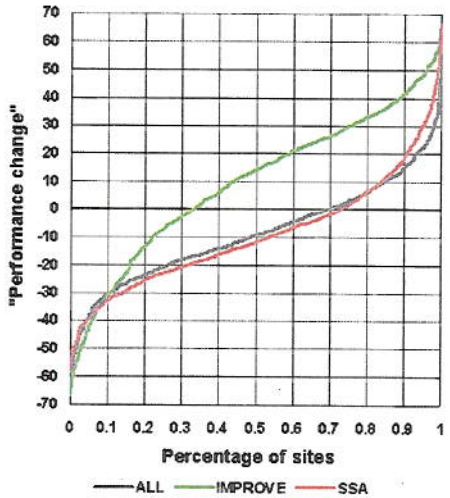

Figure S2